A multiple-component order parameter phase field model for anisotropic grain growth

M.K. Venkitachalam [a,*], L.-Q. Chen [a], A.G. Khachaturyan [b], G.L. Messing [a]

[a] *Department of Materials Science and Engineering, The Pennsylvania State University, University Park, PA 16802, USA*
[b] *Department of Materials Science and Engineering, Rutgers University, PO Box 909, Piscataway, NJ 08855-0909, USA*

Abstract

A phase field model for anisotropic grain growth is presented. The model uses multiple-component order parameters to describe the grain orientations. These order parameters are the structural amplitudes related to the star of the shortest reciprocal lattice vectors of the crystalline phase. The free energy of the system is formulated as a Landau expansion of the order parameters, which incorporates the symmetry of the crystalline phase. The spatial and temporal evolution of these order parameters is governed by the time-dependent Ginburg-Landau (TDGL) equations. In this model, the anisotropy is introduced naturally, since the effect of the underlying symmetry is taken into account in both the gradient and bulk terms in the free energy expansion. We consider a simple binary two-phase solid-liquid mixture in two dimensions with the solid having a square lattice. As an example, we studied the growth and morphology of a single solid particle in a liquid. Potential applications of the model to simulating the anisotropic grain growth in single-phase polycrystalline materials as well as in the presence of a liquid phase are discussed. © 1997 Elsevier Science S.A.

Keywords: Phase field model; Anisotropic grain growth; Ginburg-Landau equation

1. Introduction

In this work, preliminary investigations on a phase field model applicable to the simulation of anisotropic grain growth are presented. The phenomenon of anisotropic grain growth contrasts that of normal grain growth, in which the average grain size increases while the shape of the grain size distribution remains constant. Though grain growth studies were primarily oriented towards obtaining equiaxed microstructures, it has been found that deliberate introduction of anisotropic grains enhances desirable properties in some materials. For example, anisotropic grains can blunt crack tips leading to an increase in fracture toughness in ceramic materials [2]. Also, in the case of ZnO varistors, lath-like grains result in very low clamping voltages [3]. The model presented describes the morphological evolution of a crystalline solid in contact with its liquid. Hence, it is also applicable to the modeling of liquid phase sintering of ceramics.

Various factors have been suggested to cause anisotropic grain growth, which include grain boundary energy and mobility anisotropy [4,5], segregation of solutes on boundaries [6] and the presence of a liquid at the boundary [7]. Monte Carlo simulations have been applied to model anisotropic grain growth, which include both effects of interfacial energy and grain boundary mobility anisotropies [8]. Similar methods have also been used to study the effect of different shapes of Wulff plots on the nature of the resulting anisotropic microstructures [9].

Phase field models have been applied to the computer simulation of solidification, with a lot of success [10–13]. There are various methods for introducing anisotropy in a phase field model. One way to introduce anisotropy is to make the gradient energy coefficients and the mobility coefficients depend on the direction of the gradient of the order parameter [14]. Although the physical origin of the anisotropy that appears in these models is unclear, the approach successfully simulates dendritic growth with proper qualitative behavior.

Recently, one of the authors (AGK) discussed the physical origin of the long range order parameter

* Corresponding author. Fax: + 1 814 8652917.

(LRO) in computer simulation models of solidification [1]. It was shown that the simplest kinetic model of solidification is described by a multiple component order parameter, with the role of the component played by structural amplitudes related to the star of the shortest reciprocal lattice vectors of the crystalline phase. The time-dependent Ginzburg-Landau equations that govern the kinetics are derived by identifying and separating the 'slow' and 'fast' relaxing thermodynamic parameters.

The main objective of this paper is to explore the possibility of applying phase-field models to anisotropic grain growth. Following [1], a model is developed for studying anisotropic growth of a single-grain from a liquid phase, in which the anisotropy arises solely from the orientation dependence of the interfacial energy between the solid particle and the liquid. It may be pointed out that, in this model, the anisotropy arises in a natural way, since both the free energy model and the gradient energy coefficients are specific to the crystal structure being considered. As discussed by Khachaturyan [1], it is also possible to include the effect of mobility anisotropy in a rather natural way in this model.

We consider a two-component solid-liquid two-phase system. As a first attempt, we assume that the solid has the square symmetry in two dimensions. Our focus is on the shape of a single solid particle in a liquid. The possibility of applying this model to the coarsening and grain growth of many solid particles is discussed.

2. The model

We describe an arbitrary two-phase microstructure using a scalar conservation concentration field and a multicomponent nonconserved vector order parameter field. The concentration field describes the inhomogeneous concentration or composition distribution in a two-phase mixture. Within a solid particle, the value of the concentration field is equal to the equilibrium concentration in the solid and within the liquid it is equal to the liquid concentration. Across an interface between a solid particle and the liquid, the concentration varies gradually from that corresponding to the liquid to that of the solid. The values of the components of the nonconserved order parameter field are proportional to the structural amplitudes related to the star of the shortest reciprocal lattice vectors of the solid crystalline phase [1]. Therefore, they assume a value of zero within the liquid and have finite values in the solid. Similar to the concentration field, the values of the components of the nonconserved vector order parameter change continuously from zero to finite values across the interface from liquid to solid.

Within such a diffuse-interface context, the total free energy of a two-phase mixture is described by a Ginzburg-Landau form as:

$$F = \int_r f(r)\, d^3r \tag{1}$$

where the specific free energy $f(r)$ is a sum of the gradient and local terms:

$$f(r) = f_{\text{gradient}}(r) + f_{\text{local}}(r) \tag{2}$$

The local part of the free energy can be expressed as a Landau expansion over symmetry variants of the LRO parameters Φ_{H_0}. Here, Φ_{H_0} represents the set of order parameters corresponding to the set of shortest reciprocal lattice vectors. They are the coefficients in the Fourier expansion of the single particle density $\rho(r)$, as detailed in [1]. The concentration dependence of $f_{\text{local}}(r)$ will be introduced through the concentration dependence of the expansion coefficients. In order that the free energy be invariant with respect to a rigid body translation, the coefficients of the Landau expansion $A(\Phi_{H_0^1}, \Phi_{H_0^2}, ..., \Phi_{H_0^n})$ should be such that $A(\Phi_{H_0^1}, \Phi_{H_0^2}, ..., \Phi_{H_0^n}) = 0$ if $H_0^1 + H_0^2 + \cdots H_0^n \neq 0$ [15] (The set of reciprocal lattice vectors $\{H_0^1, ..., H_0^n\}$ is the set of shortest reciprocal lattice vectors for the lattice).

For the square lattice, the star of the shortest reciprocal lattice vectors consists of four vectors, $H_0^1, ..., H_0^4$ as illustrated in Fig. 1. So, following the condition for translational invariance, we formulate the local free energy as:

$$f_{\text{local}} = f_0 + A_1 (\Phi_{H_0^1} \Phi_{H_0^3} + \Phi_{H_0^2} \Phi_{H_0^4})$$

$$+ \frac{1}{4} B_1 (\Phi_{H_0^1} \Phi_{H_0^3} \Phi_{H_0^1} \Phi_{H_0^3} + \Phi_{H_0^2} \Phi_{H_0^4} \Phi_{H_0^2} \Phi_{H_0^4})$$

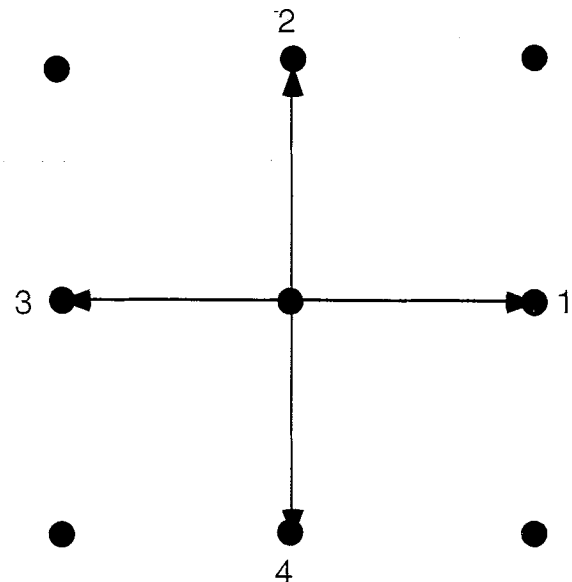$$+ \frac{1}{4} B_2 (\Phi_{H_0^1} \Phi_{H_0^3} \Phi_{H_0^2} \Phi_{H_0^4})$$

Fig. 1. For the square lattice, there are four vectors that form the star of the shortest reciprocal lattice vectors.

$$+ \frac{1}{6} C_1 ((\Phi_{H_0^1} \Phi_{H_0^3})^3 + (\Phi_{H_0^2} \Phi_{H_0^4})^3)$$

$$+ \frac{1}{6} C_2 ((\Phi_{H_0^1} \Phi_{H_0^3})^2 \Phi_{H_0^2} \Phi_{H_0^4} + (\Phi_{H_0^2} \Phi_{H_0^4})^2 \Phi_{H_0^1} \Phi_{H_0^3})$$

$$\tag{3}$$

Here, f_0 is the free energy of the liquid. Simplifying the above equation using the fact that $\Phi_{H_0^k} = \Phi^*_{-H_0^k}$ (This follows from the condition that $\rho(r, t)$ should be real), we get

$$f_{local} = f_0 + A_1(|\Phi_{H_0^1}|^2 + |\Phi_{H_0^2}|^2) + \frac{1}{4} B_1(|\Phi_{H_0^1}|^4 + |\Phi_{H_0^2}|^4)$$

$$+ \frac{1}{4} B_2(|\Phi_{H_0^1}|^2|\Phi_{H_0^2}|^2) + \frac{1}{6} C_1(|\Phi_{H_0^1}|^6 + |\Phi_{H_0^2}|^6)$$

$$+ \frac{1}{6} C_2(|\Phi_{H_0^1}|^4|\Phi_{H_0^2}|^2 + |\Phi_{H_0^1}|^2|\Phi_{H_0^2}|^4)$$

$$\tag{4}$$

For ease of notation, we replace $|\Phi_{H_0^k}|$ by η_k. Thus, the local free energy can be rewritten as:

$$f_{local} = A_1(\eta_1^2 + \eta_2^2) + \frac{1}{4} B_1(\eta_1^4 + \eta_2^4) + \frac{1}{4} B_2 \eta_1^2 \eta_2^2$$

$$+ \frac{1}{6} C_1(\eta_1^6 + \eta_2^6) + \frac{1}{6} C_2(\eta_1^4 \eta_2^2 + \eta_1^2 \eta_2^4)$$

$$\tag{5}$$

The above Landau expansion gives us four 'variants' of the square lattice at the same free energy minima, with equilibrium order parameters

$$(\eta_1, \eta_2)_{equilibrium} = (\pm \eta, \pm \eta)$$

η being a positive constant. Each one of these four solutions represents square lattices shifted from one another by one-half lattice spacing. There is no third order term in the above expansion, since in this case (i.e. square lattice) there cannot be three reciprocal lattice vectors such that $H_0^i + H_0^j + H_0^k = 0$. The sixth order term is essential for the above free energy polynomial to exhibit a first order transition.

We assume that only f_0 and A_1 in Eq. (8) depend on the concentration $c(r, t)$. The local free energy can now be written as:

$$f_{local}(c, \eta_1, \eta_2) = \frac{1}{2} A_0(c - c_1)^2 + \frac{1}{2} A_1(c - c_2)(\eta_1^2 + \eta_2^2)$$

$$+ \frac{1}{4} B_1(\eta_1^4 + \eta_2^4) + \frac{1}{4} B_2 \eta_1^2 \eta_2^2$$

$$+ \frac{1}{6} C_1(\eta_1^6 + \eta_2^6) + \frac{1}{6} C_2(\eta_1^4 \eta_2^2 + \eta_1^2 \eta_2^4)$$

$$\tag{6}$$

The coefficients in the above equation are chosen such that an equilibrium free energy-composition diagram, consistent with the phase diagram for the solid-liquid two phase system, is obtained. In this work, the constants are chosen as $A_0 = 6.0$, $A_1 = 2.5$, $B_1 = 2.5$, $B_2 = -0.5$, $C_1 = 2.5$, $C_2 = -0.5$. The free energy of the
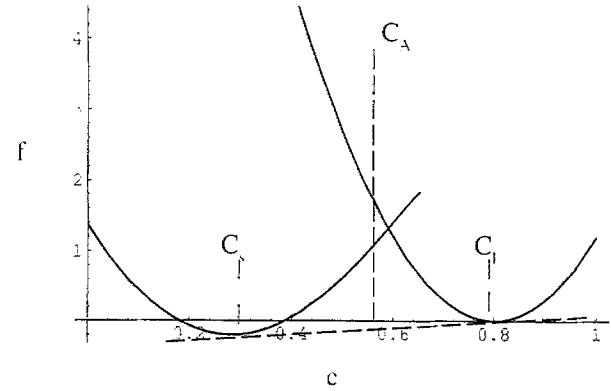

Fig. 2. Free energy (f) versus composition (c) diagram obtained from Eq. (9). The initial average composition is indicated in the figure.

liquid phase is obtained by setting all the order parametrs equal to zero. The free energy of the solid phase is obtained as follows. The local free energy in Eq. (9) is first minimized as:

$$\left. \frac{\partial f_{local}}{\partial \eta_i} \right|_{c, \eta_j, \eta} = 0 \tag{7}$$

This is a polynomial equation in η and solving this gives us the equilibrium order parameter as a function of composition. i.e.

$$\eta_{equilibrium}(c)$$

$$= \frac{\dfrac{2A_3 + A_4}{2} + \sqrt{\left(\dfrac{2A_3 + A_4}{2}\right)^2 - 4\alpha(c - c_2)(A_5 + A_6)}}{2(A_5 + A_6)}$$

$$\tag{8}$$

Substituting this back into Eq. (9) gives us the equilibrum free energy $f(c, \eta_{equilibrium}(c), \eta_{equilibrium}(c))$. The equilibrium free energy versus composition diagram is illustrated in Fig. 2.

The gradient part of the local free energy represents the excess free energy due to the presence of boundaries in the system. Here, it is expressed as:

$$f_{gradient} = \sum_i \left[\frac{\alpha}{2} (\nabla \eta_i)^2 + \frac{\beta}{2} \left(\frac{H_i \nabla \eta_i}{|H|} \right)^2 \right] \tag{9}$$

The first term represents the isotropic part of the gradients and the second, the anisotropic part, which takes into account the direction dependence of the interfacial free energy. Here η_i is the order parameter in the reciprocal lattice direction H_i/H.

Thus, the expression for the total free energy of the system is:

$$F = \int_r \left[\frac{1}{2} A_0(c - c_1)^2 + \frac{1}{2} A_1(c - c_2)(\eta_1^2 + \eta_2^2) \right.$$

$$\left. + \frac{1}{4} B_1(\eta_1^4 + \eta_2^4) + \frac{1}{4} B_2(\eta_1^2 \eta_2^2) + \frac{1}{6} C_1(\eta_1^6 + \eta_2^6) \right.$$

$$+ \frac{1}{6} C_2(\eta_1^4 \eta_2^2 + \eta_1^2 \eta_2^4)$$

$$+ \sum_i \left[\frac{\alpha}{2}(\nabla \eta_i)^2 + \frac{\beta}{2}\left(\frac{H_i \overline{\nabla \eta_i}}{|H|}\right)^2 \right]\right] d^3 r \tag{10}$$

The kinetic equations that describe the spatial and temporal evolution of the compositor variable $c(r, t)$ and the LRO parameters η_k are:

$$\frac{\partial c}{\partial t} = D\nabla^2\left(\frac{\delta F}{\delta c}\right) \tag{11}$$

and

$$\frac{\partial \eta_i}{\partial t} = -L\left(\frac{\delta F}{\delta \eta_i}\right) \tag{12}$$

Here, D is the diffusivity and L, the mobility.

The variational derivatives used in the above equations are obtained as follows:

$$\frac{\delta F}{\delta c} = \frac{\partial f_{\text{local}}}{\partial c} - \alpha(0)\nabla^2 c \tag{13}$$

$$\frac{\delta F}{\delta \eta_i} = \frac{\partial f_{\text{local}}}{\partial \eta_i} - \alpha_{kl}^{(i)}\frac{\partial^2 \eta_i}{\partial x_k \partial x_l} \tag{14}$$

here

$$\alpha_{kl}^{(i)} = \alpha\delta_{ij} + \beta\left(\frac{H_k^i H_l^i}{|H^i|^2}\right) \tag{15}$$

The anisotropy of the coefficients $\alpha_{kl}^{(i)}$ and different values of the amplitudes $\Phi_{H_0}(r)$ within the boundary layer results in the crystallographic anisotropy of the interfacial boundary. For a square lattice, the above expression results in:

$$\alpha_{kl}^{(1)} = \begin{pmatrix} \alpha+\beta & 0 \\ 0 & \alpha \end{pmatrix}, \qquad \alpha_{kl}^{(2)} = \begin{pmatrix} \alpha & 0 \\ 0 & \alpha+\beta \end{pmatrix} \tag{16}$$

Thus, the kinetic equations used for the simulation are:

$$\frac{\partial c}{\partial t} = D\nabla^2\left(\frac{\partial f_{\text{local}}}{\partial c} - \alpha(0)\nabla^2 c\right)$$

$$= D\nabla^2\left(A_0(c - c_1) + \frac{1}{2}A_1(\eta_1^2 + \eta_2^2) - \alpha(0)\nabla^2 c\right) \tag{17}$$

and

$$\frac{\partial \eta_i}{\partial t} = -L\left(\frac{\partial f_{\text{local}}}{\partial \eta_i} - \alpha_{kl}^{(i)}\frac{\partial^2 \eta_i}{\partial x_k \partial x_l}\right)$$

$$= A_1(c - c_2)\eta_i + B_1\eta_i^3 + \frac{1}{2}B_2\eta_i\eta_{i+1}^2 + C_1\eta_i^5$$

$$+ \frac{1}{6}C_2\left(4\eta_i^3\eta_{i+1}^2 + 2\eta_i\eta_{i+1}^4\right) = \alpha_{kl}^{(i)}\frac{\partial^2 \eta_i}{\partial x_k \partial x_l} \tag{18}$$

3. Simulation

The above model was used to simulate the morphological evolution of a solid in contact with a liquid. The

coefficients in the Landau polynomial were chosen such that an equilibrium free energy vs. composition diagram such as the one shown if Fig. 2 is obtained. Once the alloy composition c_A is fixed, the equilibrium volume fraction of the solid is fixed. The simulations were carried out in a square cell with 64×64 and 128×128 grid points with periodic boundary conditions along both x and y directions.

The initial conditions for the simulation are that of a circular solid particle in contact with the liquid. The size of the particle is such that the volume fraction of the solid is less than that at equilibrium. Hence, the particle grows to reach the equilibrium volume fraction and its shape can be studied by tracking the concentration and order parameter variables as a function of time.

The following discretization scheme was used for the Laplacian and gradient terms in the kinetic equations:

$$\nabla^2 c(x, y) = \left[\frac{1}{2}(c(x+\Delta, y) + c(x, y+\Delta) + c(x-\Delta, y)\right.$$

$$+ c(x, y-\Delta))$$

$$+ \frac{1}{4}(c(x+\Delta, y+\Delta) + c(x+\Delta, y-\Delta)$$

$$+ c(x-\Delta, y+\Delta) + c(x-\Delta, y-\Delta))$$

$$\left. - 3c(x, y)\right]\Big/\Delta^2 \tag{19}$$

and

$$\alpha_{kl}^{(i)}\frac{\partial^2 \eta_i}{\partial x_k \partial x_l} = [\alpha_{11}^{(i)}(\eta_i(x, y+\Delta) + \eta_i(x, y-\Delta) - 2\eta_i(x, y))$$

$$+ \alpha_{22}^{(i)}(\eta_i(x+\Delta, y) + \eta_i(x-\Delta, y)$$

$$- 2\eta_i(x, y))]/\Delta^2$$

$$+ 2\alpha_{12}^{(i)}(\eta_i(x+\Delta, y+\Delta) + \eta_i(x-\Delta, y-\Delta)$$

$$- \eta_i(x-\Delta, y+\Delta)$$

$$- \eta_i(x+\Delta, y-\Delta))]/4\Delta^2 \tag{20}$$

To visualize the growth of the solid particle, we define a function:

$$I(x, y) = \sum_{H_0} \eta_{H_0} \exp(i2\pi H_0 r)$$

$$= \eta_1 \cos(2\pi ax) + \eta_2 \cos(2\pi ay) \tag{21}$$

which goes to zero inside the liquid and attains a certain peak at any lattice position. The shape of the particle is studied by plotting $I(x, y)$ at different time steps during the simulation. This is illustrated in Fig. 3.

A convenient way of representing the particle is to plot the composition variable $c(x, y)$ at different time steps, since the equilibrium concentration of the component is different in the liquid and the solid. Such a plot is shown in Fig. 4(a). Yet another way to visualize

the kinetics is to plot $f(x, y) = \eta_1^2(x, y) + \eta_2^2(x, y)$. This is illustrated in Fig. 4(b).

The growth of a single grain was studied employing the local free energies described in Eq. (9). The initial conditions for the simulation are $\eta_1 = \eta_2 = \eta_{\text{equilibrium}}(c_s)$; $c = c_s$ within the solid and $\eta_1 = \eta_2 = 0$; $c = c_l$ inside the liquid. For each run of the simulation, the composition c_A is fixed and this fixes the equilibrium volume fraction of the solid. The initial size of the particle is less than that corresponding to this value. Hence, the particle grows to attain this volume fraction and its shape can be studied. The result of such a simulation is shown in Fig. 4(a) and (b). The order parameter and concentration profiles along a cross section of the particle are shown in Fig. 5(a) and (b). The particle shape is that of a rounded square, which is consistent with the free energy formulation in Eq. (9) and the matrix of gradient coefficients in Eq. (17). The resulting particle shape has the symmetry of the square lattice. The effect of anisotropy is small here, but that is not surprising, since the Landau expansion of the free energy is based on only the nearest neighbors in the reciprocal lattice. A discussion on how the model could be modified to allow for rotated variants of the lattice is given below.

3.1. Discussion

The local free energy in Eq. (6) is formulated by considering only the shortest reciprocal lattice vectors (nearest neighbors). Typically, an anisotropic microstructure consists of anisotropic grains of varying orientations with respect to each other. The above
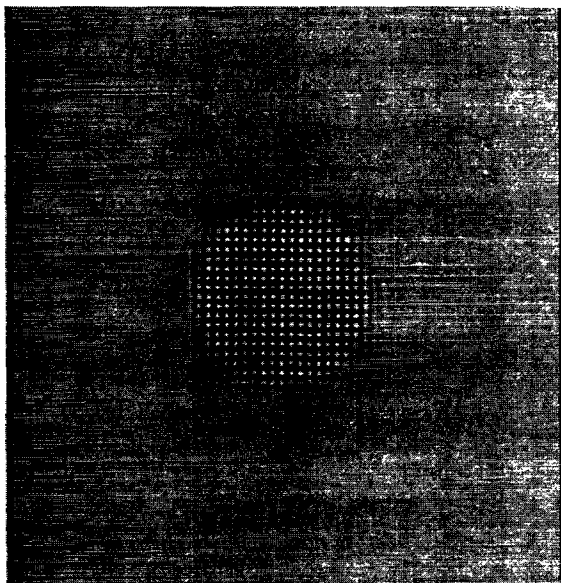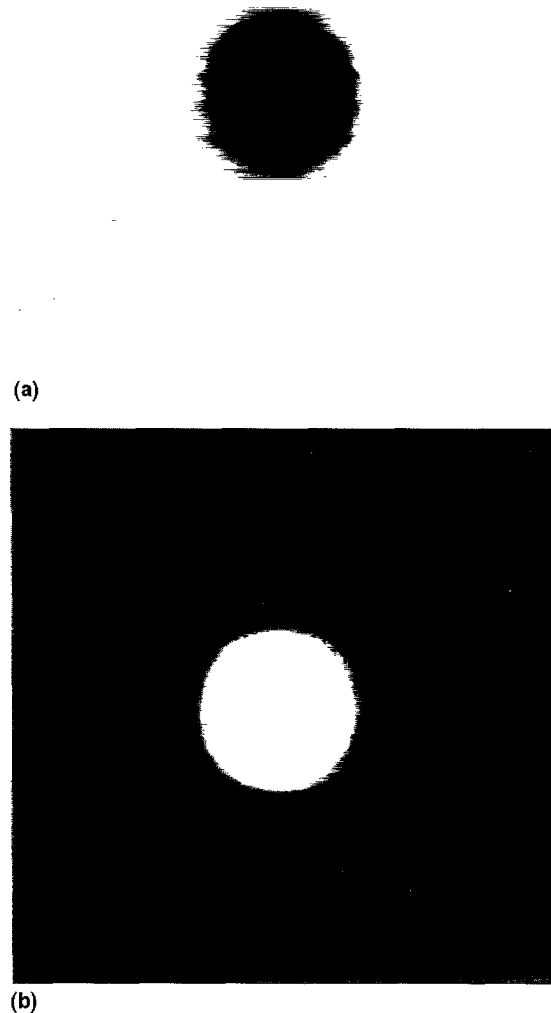

(a)

(b)

Fig. 4. (a) A plot of the concentration variable $c(x, y)$. The concentration and order parameter profiles for a cross-section through the center are shown in Fig. 5(a) and (b). The simulation is performed on a 128×128 grid. (b) An alternate way to represent the particle shape is to plot the sum of the squares of the order parameters. The simulation is performed on a 128×128 grid.

Fig. 3. The result of simulations that uses the free energy Eq. (9). (A 128×128 grid is used for the simulation).

model results in a single variant, it does not describe an anisotropic microstructure. This effect can be included in the free energy model by considering ordering along reciprocal lattice vectors in these directions. For example, in order that the local free energy give rise to three variants rotated at 30° with respect to each other, it can be formulated as follows. In this case, there are twelve order parameters (Fig. 6) and the local free energy can be written as:

$$f_{\text{local}}(\Phi_{H1}, \ldots \Phi_{H12})$$

$$= \frac{1}{2} A_1 \sum_{i=1}^{6} \phi_{Hi} \Phi_{Hi+6} + \frac{1}{3} B_1 \sum_{i=1}^{4} \Phi_{Hi} \Phi_{Hi+4} \Phi_{Hi+8}$$

$$+ \frac{1}{4} \left(C_1 \sum_{i=1}^{6} (\Phi_{Hi} \Phi_{Hi+6})^2 \right.$$

$$\left. C_2 \sum_{i=1}^{3} \Phi_{Hi} \Phi_{Hi+3} \Phi_{Hi+6} \Phi_{Hi+9} \right) \qquad (22)$$

Simplifying the above equation in the manner that Eq. (6) was simplified, we get:

$$f_{\text{local}} = \frac{1}{2} A_1 \sum_{i=1}^{6} \eta_i^2 + \frac{1}{3} B_1 \sum_{i=1}^{2} \eta_i \eta_{i+2} \eta_{i+4}$$

$$+ \frac{1}{4} \left(C_1 \sum_{i=1}^{6} \eta_i^4 + C_2 \sum_{i=1}^{3} (\eta_i \eta_{i+3})^2 \right) \qquad (23)$$

The coefficients in the above equation are chosen such that there are three sets of 'roots' at which the free energy is a minimum, each of which represents a square lattice. These variants are at 30° with respect to each other. The three sets of solutions are:

$$\{\eta\}_{\text{equilibrium}}^{(1)} = (\eta\ 0\ 0\ \eta\ 0\ 0)$$

$$\{\eta\}_{\text{equilibrium}}^{(2)} = (0\ \eta\ 0\ 0\ \eta\ 0)$$

$$\{\eta\}_{\text{equilibrium}}^{(3)} = (0\ 0\ \eta\ 0\ 0\ \eta)$$

Fig. 6. The twelve reciprocal lattice vectors used in the free energy equation which allows for rotated variants of the square lattice.

The kinetics of these order parameters are again governed by Eqs. (17) and (18), but now there would be six equations to solve for the order parameters instead of two. Using a similar approach, we could increase the number of such rotated variants. For example, to obtain six variants rotated at 15° with respect to each other, the number of order parameters would be 12. However, there would be a significant increase in the computational time due to the increase in the number of equations to be solved. The above method may hence be applied to simulate the evolution of an anisotropic microstructure with grains at different orientations.

4. Summary

A model has been developed, which uses multiple order parameters in a phase field model to describe the anisotropic growth of a crystal from its liquid. An extension of the same method, which allows for the inclusion of rotated variants of the crystalline lattice, is also discussed. Once the rotations are allowed for, the above model can be applied to simulate anisotropic grain growth. It can also be applied to study the morphological evolution during liquid phase sintering of ceramics.

The focus of the current work was on formulating a specific free energy model using the general theory described in [1] for a simple lattice, and performing simulations on the growth of such a crystal from its liquid. The next step would be to calculate the energy of an interface as a function of the interface orienta-
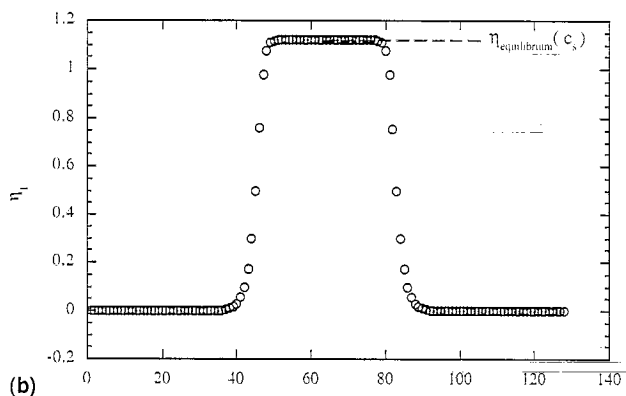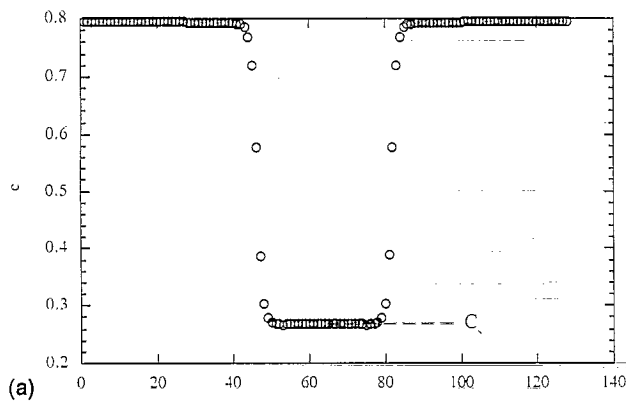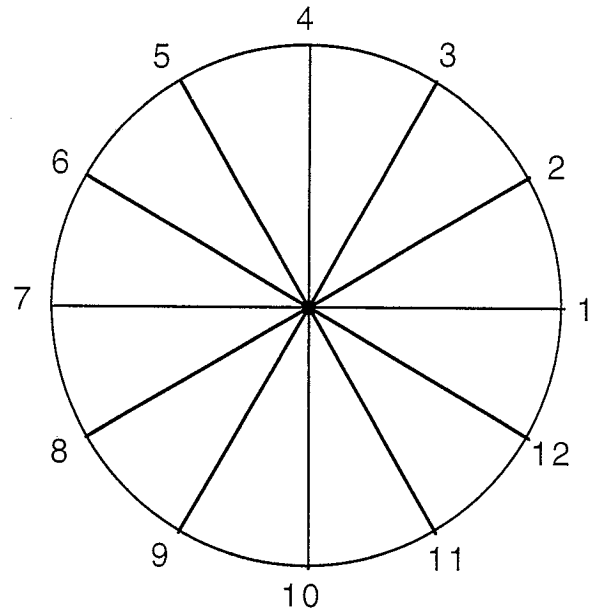

Fig. 5. (a) Concentration profile across the particle shown in Fig. 4(a). (b) Order parameter profile across the particle shown in Fig. 4(a).

tion. Such calculations have been performed on phase field models for antiphase boundaries [16,17]. The model can also readily be extended to three dimensions, though this would make the computation much more time intensive.

Acknowledgements

References

[1] A.G. Khachaturyan, Phil. Mag. A74 (1996) 3.

[2] K.T. Faber, A.G. Evans, Acta Metall. 31 (1988) 469.

[3] L.T. Bowen, F.J. Avella, J. Appl. Phys. 54 (1983) 2764.

[4] A.H. Heuer, G.A. Fryburg, L.U. Ogbuji, T.E. Mitchell, S. Shinozaki, J. Am. Ceram. Soc. 61 (1978) 406.

[5] T.E. Mitchell, L.U. Ogbuji, A.H. Heuer, J. Am. Ceram. Soc. 61 (1978) 412.

[6] S.J. Bennison, M.P. Harmer, J. Am. Ceram. Soc. 66 (1983) C-90.

[7] W.A. Kaysser, M. Sprissler, C.A. Handwerker, J.E. Blendell, J. Am. Ceram. Soc. 70 (1987) 339.

[8] A.D. Rollett, D.J. Srolovitz, M.P. Anderson, Acta Metall. 57 (1989) 1227.

[9] W. Yang, G.L. Messing, L.-Q. Chen, Mater. Sci. Eng. A195 (1995) 179.

[10] A.A. Wheeler, W.J. Boettinger, G.B. McFadden, Phys. Rev. A45 (1992) 7424.

[11] A.A. Wheeler, W.J. Boettinger, G.B. McFadden, Phys. Rev. E47 (1993) 1893.

[12] G. Caginalp, W. Xie, Phys. Rev. E48 (1993) 1897.

[13] J.A. Warren, W.J. Boettinger, Acta Metall. Mater. 43 (1995) 689.

[14] R. Kobayashi, Physica D63 (1993) 410.

[15] A.G. Khachaturyan, The Theory of Phase Transformations in Solids, Wiley, New York, 1983.

[16] R.J. Braun, J.W. Cahn, J. Hagedorn, G.B. McFadden, A.A. Wheeler, Mathematics of Microstructural Evolution, TMS, 1996.

[17] J.E. Kraznowski, S.M. Allen, Surf. Sci. 144 (1984) 153.